

Analyzing and Simulating Fracture Patterns of Thera Wall Paintings

HIJUNG SHIN, Princeton University

CHRISTOS DOUMAS, National University of Athens and Akrotiri Excavation

THOMAS FUNKHOUSER, SZYMON RUSINKIEWICZ, and KENNETH STEIGLITZ, Princeton University

ANDREAS VLACHOPOULOS, University of Ioannina and Akrotiri Excavation

TIM WEYRICH, University College London

In this article, we analyze the fracture patterns observed in wall paintings excavated at Akrotiri, a Bronze Age Aegean settlement destroyed by a volcano on the Greek island of Thera around 1630 BC. We use interactive programs to trace detailed fragment boundaries in images of manually reconstructed wall paintings. Then, we use geometric analysis algorithms to study the shapes and contacts of those fragment boundaries, producing statistical distributions of lengths, angles, areas, and adjacencies found in assembled paintings. The result is a statistical model that suggests a hierarchical fracture pattern where fragments break into two pieces recursively along cracks nearly orthogonal to previous ones. This model is tested by comparing it with simulation results of a hierarchical fracture process. The model could be useful for predicting fracture patterns of other wall paintings and/or for guiding future computer-assisted reconstruction algorithms.

Categories and Subject Descriptors: J.5 [Arts and Humanities]; I.5.1 [Pattern Recognition]: Models; I.6.4 [Simulation and Modeling]: Model Validation and Analysis

General Terms: Measurement

Additional Key Words and Phrases: Statistical modeling, hierarchical fracture, cultural heritage

ACM Reference Format:

Shin, H., Dumas, C., Funkhouser, T., Rusinkiewicz, S., Steiglitz, K., Vlachopoulos, A., and Weyrich, T. 2012. Analyzing and simulating fracture patterns of Thera wall paintings. *ACM J. Comput. Cult. Herit.* 5, 3, Article 10 (October 2012), 14 pages. DOI = 10.1145/2362402.2362404 <http://doi.acm.org/10.1145/2362402.2362404>

1. INTRODUCTION

Reconstruction of fractured ancient artifacts such as frescoes, pots, statues, and tablets is important because it helps archaeologists make inferences about past civilizations and cultures. Unfortunately, reconstruction is usually a painstakingly labor-intensive job which may take several months or even years to complete by hand if the number of fragments is very large.

To overcome this problem, several computer scientists have worked on automated reconstruction systems that acquire photographs and/or close-range 3D laser scans of fragments and then use computer algorithms to assemble them [Willis and Cooper 2008]. Example projects of this type include

Author's address: H. Shin (corresponding author), Princeton University, Princeton, NJ; email: hishin@mit.edu.

Permission to make digital or hard copies of part or all of this work for personal or classroom use is granted without fee provided that copies are not made or distributed for profit or commercial advantage and that copies show this notice on the first page or initial screen of a display along with the full citation. Copyrights for components of this work owned by others than ACM must be honored. Abstracting with credit is permitted. To copy otherwise, to republish, to post on servers, to redistribute to lists, or to use any component of this work in other works requires prior specific permission and/or a fee. Permissions may be requested from Publications Dept., ACM, Inc., 2 Penn Plaza, Suite 701, New York, NY 10121-0701 USA, fax +1 (212) 869-0481, or permissions@acm.org.

© 2012 ACM 1556-4673/2012/10-ART10 \$15.00

DOI 10.1145/2362402.2362404 <http://doi.acm.org/10.1145/2362402.2362404>

Stitch [Cooper et al. 2001] and Forma Urbis Romae [Koller and Levoy 2006]. They typically use combinatorial algorithms to search for the arrangement of fragments that optimizes a scoring function, usually designed heuristically based on the compatibility of properties in adjacent fragments. While they have demonstrated some success, they still are not able to assemble complete artifacts from many fragments automatically [Willis and Cooper 2008].

In this article, we utilize analysis of previously reconstructed wall paintings to learn the statistics of correct fragment arrangements. Our goal is to gather data that can be used to characterize the arrangements of fragments typically found in reconstructions so that more principled scoring functions can be developed and generative models of crack formation can be evaluated. We use interactive programs to trace detailed fragment boundaries in images of manually reconstructed wall paintings containing approximately 4,000 fragments. Then, we use geometric analysis algorithms to study the shapes and contacts of those fragment boundaries, producing statistical distributions of lengths, angles, areas, and adjacencies found in assembled arrangements of fragments.

These statistics reveal information that could guide future scoring functions and/or generative models. Loosely speaking, we find that (1) fragments tend to be nearly convex polygons, (2) the distribution of fragment areas roughly follows an exponential distribution, (3) cracks between fragments tend to be nearly straight, and (4) cracks most often meet at right angles.

These observations support the hypothesis that the cracks formed as the result of a hierarchical process where fragments were broken recursively into two subfragments along nearly straight cracks are nearly orthogonal to previous cracks. We confirm this hypothesis by performing simulations of hierarchical fracture processes and then comparing their statistics with the ones observed from the actual fresco. Investigating a model of a fracture process with statistical analysis of continuous-valued properties of reconstructed wall paintings is the most novel contribution of our work.

2. RELATED WORK

There has been a long history of work on computer-aided reconstruction of fractured objects in archaeology [Kleber et al. 2009; Willis and Cooper 2008]. Most previous work has focused on finding pairwise matches between adjacent fragments by aligning patterns in their surface colors [Papaodysseus et al. 2008], polygonal boundaries [Papaodysseus et al. 2002; Leitão and Stolfi 2002], normal maps [Toler-Franklin et al. 2010], and/or fractured edges [Brown et al. 2008; Huang et al. 2006; Papaioannou and Karabassi 2003]. These methods have been successful in cases where the fragments have highly distinctive features [Huang et al. 2006], the reconstructed objects are surfaces of revolution [Karasik and Smilansky 2008]), and/or when domain-specific features can be used to identify potential matches [Koller and Levoy 2006]. However, they have not been able to automatically reconstruct archaeological artifacts with a multitude of flat, partially eroded fragments [Willis and Cooper 2008].

There are two significant problems. First, it is intractable to exhaustively search the space of potential fragment alignments [Demaine and Demaine 2007]. Second, it is difficult to devise a “scoring function” that effectively discriminates correct alignments from incorrect ones. As a result, most prior reconstruction algorithms have employed heuristics to prune the search space based on expected relationships between adjacent fragments. For example, in the domain of jigsaw puzzle solving [Freeman and Garder 1964], the boundary of each piece can be partitioned robustly into discrete features representing “tabs,” “indents,” “corners,” and “border edges,” and only certain types of arrangements are possible when joining those features (e.g., corners abut with corners, tabs align with indents, border edges continue across several pieces, etc.). Thus, it is possible to prune the space of potential matches significantly, and puzzles with up to 200 pieces can be solved [Goldberg et al. 2004]. Our goal is to

generalize these methods to the domain of wall painting reconstruction where relationships between adjacent fragments are not so clear-cut and thus must be described statistically.

Statistical analysis of fracture patterns has a long history in mechanics [Griffith 1921], geology [Cloos 1955], forensics [McDanel et al. 2006], paleontology [Bhandarkar et al. 2009], and several other fields. In 1962, Lachenbruch [1962] classified fracture patterns as either orthogonal (e.g., hierarchical) or nonorthogonal (e.g., hexagonal). He observed that junctions are often at right angles in orthogonal structures. In 1968, Rats [1968] proposed a “rule of identical areas” suggesting that stone blocks break into nearly equally-sized pieces until a minimum block size is reached and observed that orthogonal fracture patterns have predominantly four-sided fragments. Mulheran [1993] observed that crack networks in thin films are statistically self-similar, suggesting that fragment areas have an exponential distribution. Other specialists have studied hierarchical fracture patterns in ceramics [Kornetta et al. 1998], chalk [Cawsey 1977], clay [Tang and Shi 2008], polymer coatings [Handge 2002], mud [Bohn et al. 2005], and other materials.

Within archaeology, there have been a few projects aimed at fracture pattern analysis. Leitão and Stolfi [2005] studied the information content in fracture contours with the goal of understanding whether reconstruction of artifacts with many fragments is theoretically possible. McBride and Kimia [2003] studied types of edges and joints in fractured frescoes, observing that the vast majority of junctions appear where three fragments join in a “T” junction (70–89%) and that discernable corners in fragment contours usually align in pairwise fragment matches (77–78% have at least one corner aligned). The authors utilized these observations in a reconstruction algorithm that considered only pairwise matches that align corners, demonstrating results for test datasets with 13–25 fragments. While this work takes a significant first step in the direction of our article, it provides only very coarse statistics (i.e., counts of the number of junctions falling into certain predefined cases). It does not study traced boundaries of fragments and/or gather continuous-valued descriptions of how fragments are arranged (e.g., areas, lengths, angles, etc.), and it does not advocate a specific model of the fracture process and/or use simulations to compare fracture patterns, and thus the statistical analysis and range of applications are not as general as ours.

This article provides results for simulated and real data, while additional details about analyzing fracture patterns are shown in Shin et al. [2010]. The main difference is the addition of a simulation study (Section 5). This article is also related to Funkhouser et al. [2011], which leverages the analysis herein to derive new features for matching fragment contours.

3. METHODS

The main contribution of our work is the development a statistical model for the crack pattern of a fractured wall painting. Starting from a high-resolution image of a manually reconstructed fresco, we use an interactive program of our own design to trace contours around every fragment in the image and then gather statistical distributions of spatial properties that characterize the observed arrangement of fragments. These statistics form a data-driven probabilistic model for the fracture pattern. We confirm this model using simulations produced by the Berkeley Surface Cracking Toolkit [Iben and O’Brien 2009].

Our test case is a wall painting called “Crocus Gatherer and Potnia” (top left of Figure 1), which was recovered from the Xeste 3 building at the archaeological site of Akrotiri, Thera. This was a Late Bronze Age settlement destroyed circa 1630 B.C. by a volcanic eruption, preceded by strong earthquakes. The settlement, well preserved by volcanic ash, has been the site of an excavation since 1967, and dozens of wall paintings have been recovered and are being reassembled [Doumas 1992].

The wall paintings were constructed on an interior wall that was covered first by mud and straw, then by a layer of lime plaster roughly 1 cm thick. The designs, which include both *buon fresco* and

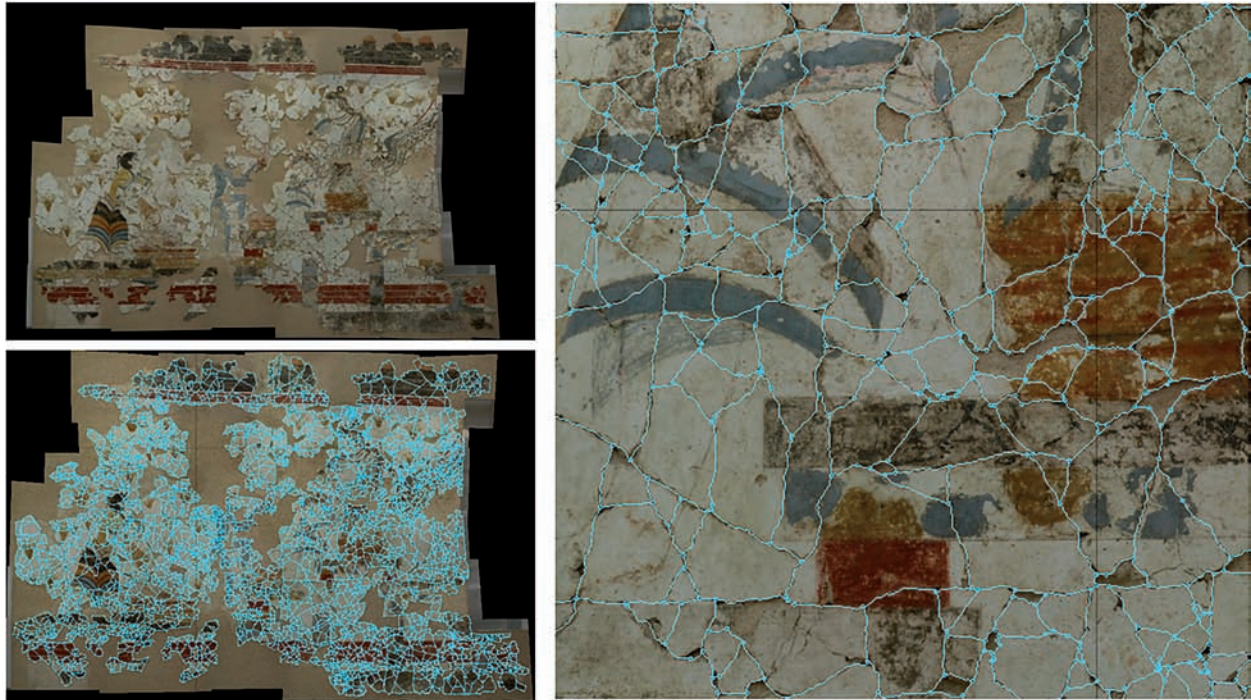


Fig. 1. High-resolution color image of a reconstructed Thera wall painting called *Crocus Gatherer and Potnia* (republished with permission from Figs 122–128 of “The Wall Paintings of Thera” [Doumas 1992]). The painting (3.22×2.30 meters) was photographed at 80 pixels per centimeter by George Papandreou [Papandreou 2009] (top left), and then every fragment was outlined with a contour tracing program to yield a polygonal mesh representation (bottom left) with 4,147 fragments, including 156 gaps, 10,994 edges (blue lines), and 4,921 junctions. A zoomed view of the polygonal mesh is shown on the right. (Copyright: Akortiri Excavations, Thera).

fresco secco areas, were applied to a final thin layer of fine plaster [Doumas 1992]. The wall paintings are excavated in thousands of small fragments, cleaned and conserved, then manually reassembled by skilled curators over the course of many years.

The Potnia (Goddess of Nature of the Bronze Age Aegean societies) was found scattered in hundreds of fragments in the interior of Xeste 3 (Room 3a), and archaeological study has shown that it decorated the north wall of this space on the second floor of the building [Vlachopoulos 2007]. Both the north wall of Room 3a and the wall painting collapsed, and the restoration of the composition (comprising another *Crocus Gatherer* proceeding from the right and an oblong window between her and the Potnia) took more than 10 years. In this article, we focus on the left part where a young girl empties her basket with crocus flowers in a pannier, from which a blue monkey takes a posy of dried stamens and offers them to the seated Potnia. This part measures 3.2m in width and 2.3m in height, and we work with a high-resolution image produced by stitching together a large number of digital photographs [Papandreou 2009].

Our article describes a processing pipeline to analyze the fracture patterns in the “potnia” and other wall paintings. The following two sections describe the main steps of this processing pipeline: contour tracing and contour analysis. The result of this analysis is a statistical model of the fracture process (Section 4). This model is confirmed using a simulation in Section 5. Finally, Section 6 provides a summary of our findings and topics for future work.

3.1 Contour Tracing

Beginning with a high-resolution color image of a manually reconstructed fresco (top left of Figure 1), our first goal is to trace the contour outlining the perimeter of every fragment (bottom left of Figure 1). This goal is challenging because a single fresco may have thousands of fragments and the cracks between those fragments may form a complex network of contours, requiring millions of points to capture the paths of all cracks accurately.

Ideally, we could write a computer program that would extract fragment contours from a color image automatically. However, cracks are difficult to detect robustly, especially in painted regions where crack patterns are intermixed with color patterns [Bazin and Henry 2003]. As a result, it is difficult for a computer to discover the topology and gross placement of contours completely automatically, as there are many situations in which the global structure of the fracture pattern must be understood in order to determine the correct placement and connectivity of junctions (a task that people are very good at). Alternatively, we could ask a person to trace every contour with an interactive tracing program. However, it would be tedious and error-prone for a person to trace the path of every crack accurately (at pixel precision) since cracks typically have many slight changes in direction that would be difficult to trace interactively (a task that computers are good at). So, we take a hybrid approach.

We have implemented a semi-automatic program to trace fragment boundary contours inspired by the “intelligent scissoring” approach of Mortensen and Barrett [1995]. The user begins by clicking on a junction or other point of interest. Then, as he or she moves the mouse away from the clicked “anchor” point, the computer interactively displays the optimal computed path between the anchor and the current cursor position. The user may click to place another anchor point, freezing the current curve, or click on a previously placed curve or anchor, joining the curve to a newly created junction.

The optimal path minimizes an energy function designed to snap to cracks in the image. Because the cracks appear darker than the surrounding plaster, we define the energy function \mathcal{E} at each pixel to be smaller when the pixel’s intensity is lower than its neighbors’. Specifically, we minimize the following error function, which favors shorter paths along darker pixels:

$$\mathcal{E}(p) = [1 + I(p) - \max_{q \in \mathcal{N}(p)} I(q)]^n. \quad (1)$$

The exponent n is used to determine the strength of snapping: lower values favor short paths, while higher ones allow the path to deviate more from a straight line in order to follow cracks (we found that $n = 8$ provides a reasonable trade-off). Since the error function grows monotonically along a path, Dijkstra’s algorithm can be used to efficiently find optimal paths at interactive rates.

The bottom-left and rightmost images in Figure 1 show screenshots of the program after the contour tracing process is complete. The tracing process for this result took approximately 20 hours of user input. Note that while cracks are treated as infinitely thin lines, they are not. Due to erosion, chipping, and deformation, gaps may be introduced between fragments. Therefore the accuracy of our results depends on the resolution with which we click “anchor” points and trace contours. For example, what looks like a four-or five-way junction in low resolution may turn out to be, in higher resolution, several three-way junctions clustered together. For this reason, we use a high-resolution image (80 pixels per cm) and try to achieve maximum resolution during contour tracing, resolving higher-order junctions as much as possible.

The result is a polygonal mesh covering the image where each polygon represents a fragment or gap (marked by the user), each edge represents a sequence of points along the boundary between two fragments (shown in blue), and each vertex represents a junction at a position where multiple edges/fragments meet. Since junctions and edges contain points shared between fragments, topological

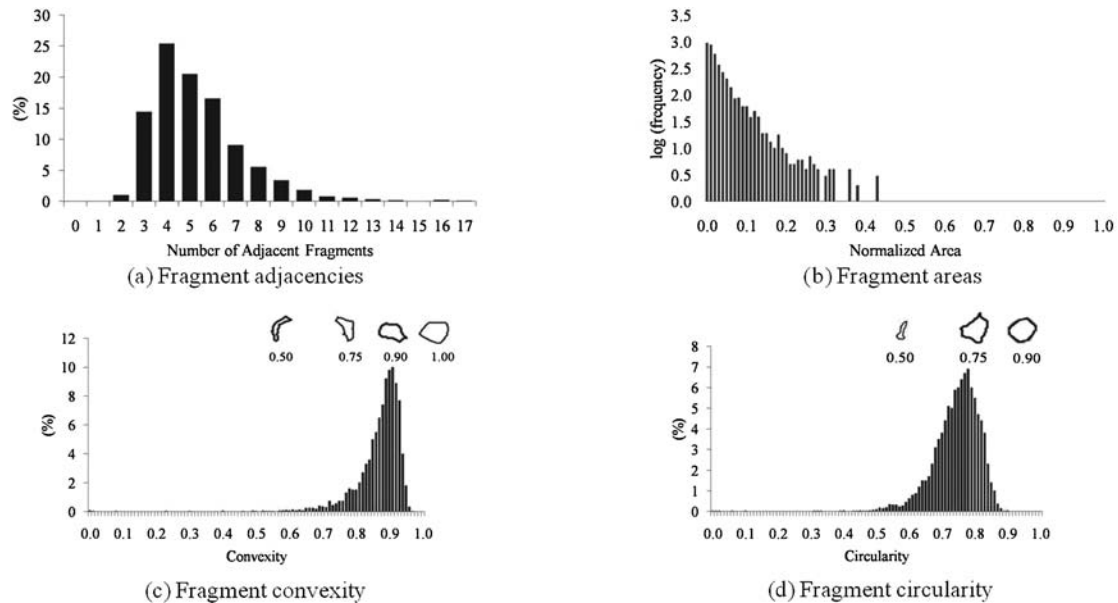


Fig. 2. Histograms of fragment properties.

adjacencies and geometric properties (e.g., angles, lengths, and areas) are easily computed from the polygonal mesh.

3.2 Contour Analysis

Once we have a polygonal mesh output by the contour tracing program, we analyze its geometric and topological properties with the goal of building a statistical model of its crack pattern. Specifically, we investigate properties of fragments (adjacencies, area, convexity, and circularity), edges (lengths, angles, straightness, and corner types), and junctions (adjacencies, angles, and corner types). We present statistics gathered during our analysis in this section and discuss a possible model of fracture process suggested by these observations in the next section.

Fragment Adjacency. Figure 2(a) shows a histogram of the number of fragments adjacent to each fragment. Two fragments are adjacent to each other if they share one or more boundary points (i.e., if they have a common edge). We only consider interior fragments (ones that are not adjacent to a gap). We observe that most fragments are adjacent to 3–8 other fragments, and the mode is four. However, there are a few small fragments surrounded by two fragments and a few large fragments adjacent to more than ten.

Fragment Area. Figure 2(b) shows a histogram of fragment areas plotted on a log scale. The histogram is normalized to $(0,1]$. The observed distribution seems to roughly follow an exponential distribution with many small fragments and few large ones.

Fragment Convexity. Figure 2(c) shows a histogram of fragment convexity, computed as the area of the fragment divided by the area of its convex hull. Representative examples for four different convexity values are inset along the top of the histogram. This distribution indicates that the vast majority of fragments are almost, but not perfectly, convex. We observe that deviations from perfect

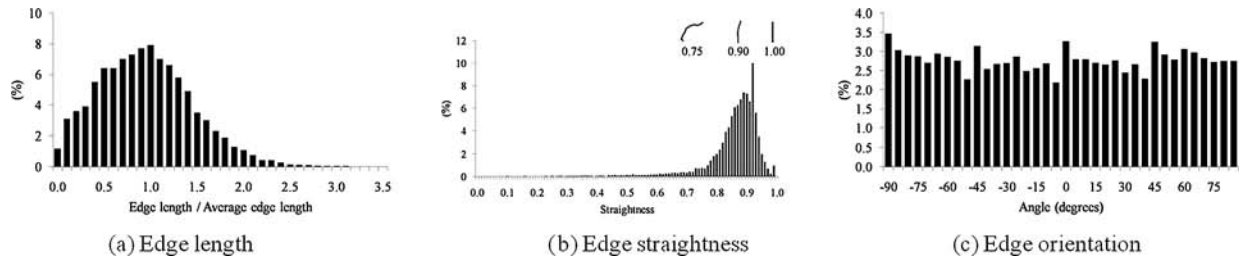


Fig. 3. Histograms of edge properties.

convexity are mainly due to small concavities that form along edges that are not completely straight (rather than a few deep concavities amongst perfectly straight edges), as shown in the inset examples.

Fragment Circularity. Figure 2(d) shows a histogram of fragment circularity, computed as $\sqrt{4 * \pi * area / perimeter}$. The circularity measure provides a value between zero (line segment) and one (perfect circle) indicating how “round” the fragment is, as shown in examples inset across the top of the figure. From the histogram, we observe that fragments rarely have extremely elongated or almost perfectly circular shapes like the examples shown on the left and right, but rather tend to have circularities like a nearly regular 4–6-sided polygon like the example shown in the middle.

Edge Length. Figure 3(a) shows a histogram of edge lengths (normalized by the average edge length of its fragment). This distribution shows a peak near the value one, which shows that most edges of the same fragment have approximately the same lengths. Edges of a perfectly regular polygon would provide a value of exactly one.

Edge Straightness. Figure 3(b) shows a histogram of edge Straightness is computed by dividing the length of the straight line segment between the two adjacent junctions by the length of the path following the sequence of points along the edge. This measure has values between zero (loop) and one (line segment) indicating how much the edge path deviates from a straight line. We see that the majority of edges are almost straight (65% have straightness above 0.9). However, some edges are highly curved (e.g., straightness below 0.5), possibly due to inhomogeneities in the wall materials.

Edge Orientation. Figure 3(c) shows a histogram of edge orientation, the counterclockwise angle in degrees between an edge’s vector \vec{v} and the positive X axis, where the edge’s vector \vec{v} spans the positions of the two adjacent junctions). Although one might think that edges would have dominant orientations correlated with the angles of support structures and the directionalities of destructive forces. However, we observe no strong preference for any particular crack direction (small peaks at multiples of 45 degrees are probably due to discretization of measurements on the pixel image).

Edge Type. Figure 4 shows the distribution of edge types defined by McBride and Kimia [2003]. Pairs of adjacent fragments are classified into three different types depending on how fragment corners align, where corners are defined as points on the boundary of a fragment where the contour bends abruptly by more than 45 degrees. In 14.9% of the edges (type 1), two corners on each fragment align at junctions delimiting the edge. In 44.3% of edges (type 2), one corner on each fragment aligns at a junction. The remaining 40.8% (type 3) have no corners aligned. These results are roughly similar to the ones reported by McBride and Kimia [2003].

Junction Angles. Figures 5(a)–5(b) show distributions of interior angles formed by adjacent edges at junctions. For each junction adjacent to K edges, there are K interior angles formed by pairs of adjacent

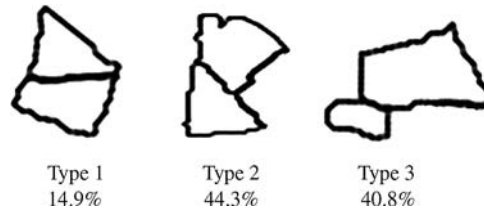


Fig. 4. Frequencies of edge types (as defined in [McBride and Kimia 2003]).



Fig. 5. Histograms of junction angle properties.

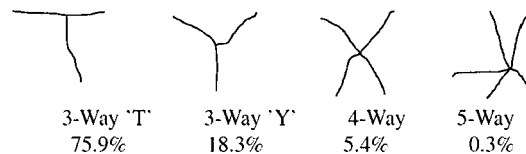


Fig. 6. Frequencies of junction types.

edges (i.e., corner angles of the adjacent fragments). We compute the measure for each of these angles by forming vectors from the junction position to a point 1/3 of the way along the two adjacent edges and then measuring the angle between those vectors (see inset in Figure 5(b)). We find the minimum and maximum interior angle at each junction and include them into the histograms shown in Figures 5(a) and 5(b), respectively. Note that the distribution of minimum angles is centered around 80–90 degrees, while the maximum angles are centered around 140–160 degrees.

Junction Type. Figure 6 shows the distribution of observed junction types. A junction is labeled “K-way” if it has K adjacent fragments/edges. For 3-way junctions, we call it a “3-way T” if its maximum interior angle is between 135 and 225 degrees, that is, if two of its three edges almost form a straight line. Otherwise, we call it a “3-way Y”. It is interesting to note that we observe only 3-way, 4-way, and 5-way junctions. Among these the vast majority are 3-way junctions (94%), and most of them are “3-way T”s (76%). These results are roughly consistent with those of McBride and Kimia [2003].

4. HIERARCHICAL FRACTURE MODEL

The statistics presented in the previous section suggest several points about the process by which the wall painting fractured.

—The predominance of 3-way “T” junctions suggest a sequential fracture process, whereby a crack forms and propagates until it collides with a previously formed crack. The predominance of

right-angle junctions provide further evidence of this sequential process as each crack propagates in the direction orthogonal to the boundary of the fragment being cracked. (The direction that optimally relieves load is orthogonal to the fragment boundary [Lachenbruch 1962].)

- The exponential distribution of fragment areas (Figure 2(b)) suggests a hierarchical fracture process where fragments are broken recursively into statistically self-similar patterns. Similar distributions of fragment areas have been observed in hierarchical fracture processes for mud [Tang and Shi 2008], ceramics [Kornetta et al. 1998], thin films [Mulheran 1993], and polymer coatings [Handge 2002].
- The distributions of fragment adjacency (Figure 2(a)), fragment convexity (Figure 2(c)), and edge straightness (Figure 3(b)) suggest that most fragment boundaries can be well-approximated by a convex polygon with a small number of sides (3–8). The predominance of four-sided fragments has been observed in hierarchical fracture processes for stone [Tsygankov 2000] and desiccated gels [Bohn et al. 2005].
- The distributions of edge lengths (Figure 3(a)) and fragment area, convexity, and circularity (Figure 2(b)–2(d)) suggest that hierarchical cracks tend to split fragments into subfragments with nearly equal areas. To produce a hierarchical sequence of nearly convex and regular polygons, cracks tend to form across the shortest dimension of each fragment, splitting it in two with almost equal length sides and high circularity. This observation is supported by the “rule of identical areas,” which was previously proposed for the fracture of stone [Rats 1968].

Based on the combination of these observations, we conjecture that the “Crocus Gatherer and Potnia” was fractured by a sequential, hierarchical process where brittle fragments broke recursively into two nearly equal-size pieces along cracks nearly orthogonal to previous ones.

5. SIMULATION

We use simulation in order to collect further evidence for this hierarchical fracture model. Our approach is to simulate fracture patterns and compare it with the ones from “Crocus Gatherer and Potnia.” Specifically, we use the Berkeley Surface Cracking Toolkit described in Iben and O’Brien [2009] to model a hierarchical fracture process. This software generates crack patterns based on physical principles. It takes in as inputs a triangle discretization of a surface, a material strength field, and an initial stress field. The cracks are produced by evolving the initial stress field over time.

Our input is a triangular mesh of a flat surface that matches the aspect ratio of the “Potnia.” We use a brittle material with an irregular strength field to model inhomogeneities such as pebbles that are found in the “Potnia” wall painting. Finally, we simulate a situation in which the fresco is hit by diverse forces at multiple points of impact. (Imagine, e.g., a fresco breaking as the wall wobbles and collapses.) We believe this is a reasonable scenario but further investigation is required to know exactly what type of force was acting on the fresco at the time of its fracture. We found that a maximum of 3,000 crack iterations produce about the same number of fragments (3,000–5,000 fragments) as the “Potnia”.

Figure 7 (left) shows a part of the fracture pattern produced by the simulation. As the comparison with the patterns observed in the “Potnia” (7 right) demonstrate, the simulation generates fracture patterns that are similar to actual cracks. In the following text, we present statistics gathered from the simulation results overlaid with the statistics from Section 3.2.

Fragment Properties. Figures 8(a)–8(d) show histograms of the fragment properties of the simulation (red), compared to those of the *Crocus Gatherer and Potnia* (black). The small number of adjacent fragments (3–8) and the exponential distribution of fragment areas are consistent with the data from the *Potnia* as well as observations from other hierarchical fracture processes [Tang and Shi 2008; Tsygankov 2000]. The fragments produced by the simulation are also highly convex and circular like the

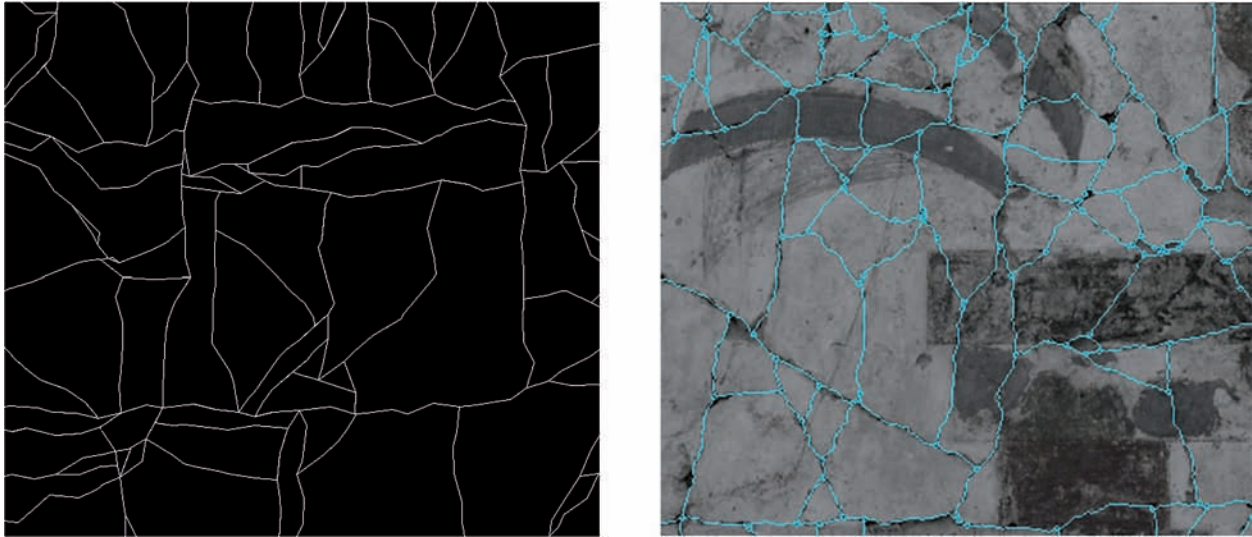


Fig. 7. Fracture patterns produced by the Berkeley Surface Cracking Toolkit [Iben and O’Brien 2009] (left), and from the *Crocus Gatherer and Potnia*, (right).

ones from the *Potnia*. However, there is a shift toward even more perfectly convex fragments. We observe that this difference can be attributed to straighter edges (see also Figure 9(b) below), and we believe edge straightness is affected by the mesh resolution, which defines the coarsest unit by which a crack can vary direction.

Edge Properties. Figures 9(a)–9(d) show the edge properties of the simulation compared to the “*Potnia*”. Like the *Potnia*, edges of the same fragment in our simulation have approximately the same lengths, and they are evenly distributed along all directions. The distribution of edge straightness is also roughly similar to the ones observed in the “*Potnia*” with the exception that there are more almost perfectly straight edges. As mentioned before, we believe this difference is due to the discrete nature of the simulation, which favors cracks following existing edges of the mesh.

Junction Properties. Figures 10(a)–10(c) compare distributions of minimum and maximum interior angles formed at junctions, and junction types. The distributions of minimum and maximum angles in our simulation are roughly similar to those observed in the “*Potnia*”. However, the maximum angles are shifted slightly toward 180 degrees. We believe this shift is produced due to the bias in the edge angles of the input mesh. The simulation favors cracks aligned with edges of the input mesh by snapping cracks to edges if angles between them are less than a threshold. Similarly, it is more likely to produce junctions aligned with vertices in the input mesh, which explains the greater number of non-3-way junctions in the simulation. Nonetheless, note that the majority of junctions are 3-way junctions (80.0%), specifically “3-way T”s (73.1%). This result is roughly consistent with those observed from the “*Potnia*” and McBride and Kimia [2003].

In general, the statistics observed from the simulation of a hierarchical fracture process agree with the ones from the wall painting, providing further support for this model as a possible fracture process of the Theran wall paintings. This fracture model has been described in Lachenbruch [1962] and

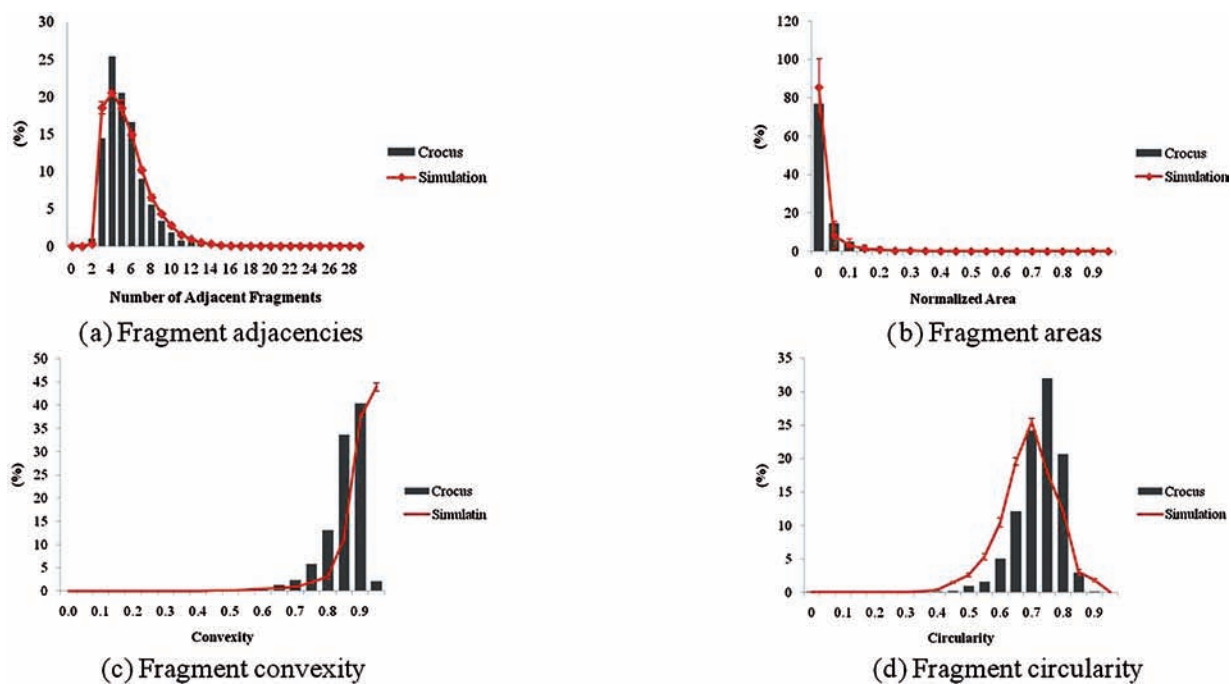
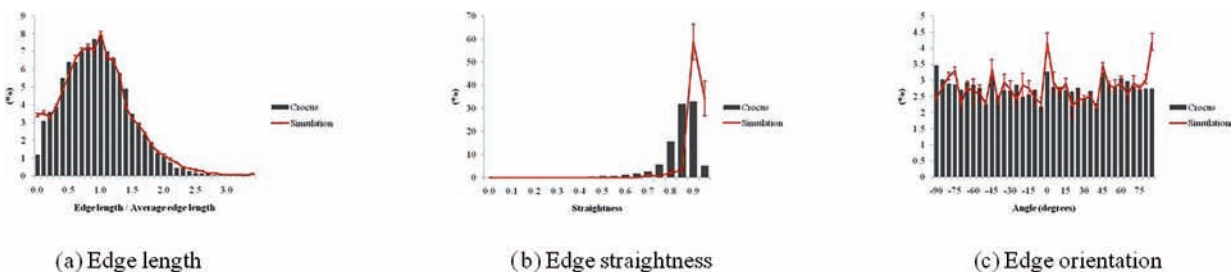


Fig. 8. Comparison of fragment properties.



Edge Type	Type 1	Type 2	Type 3
Data Set			
Crocus	14.9%	44.3%	40.8%
Simulation	6.9%	34.1%	59.0%

(d) Edge types (as defined in McBride and Kimia 2003)].

Fig. 9. Comparison of edge properties.

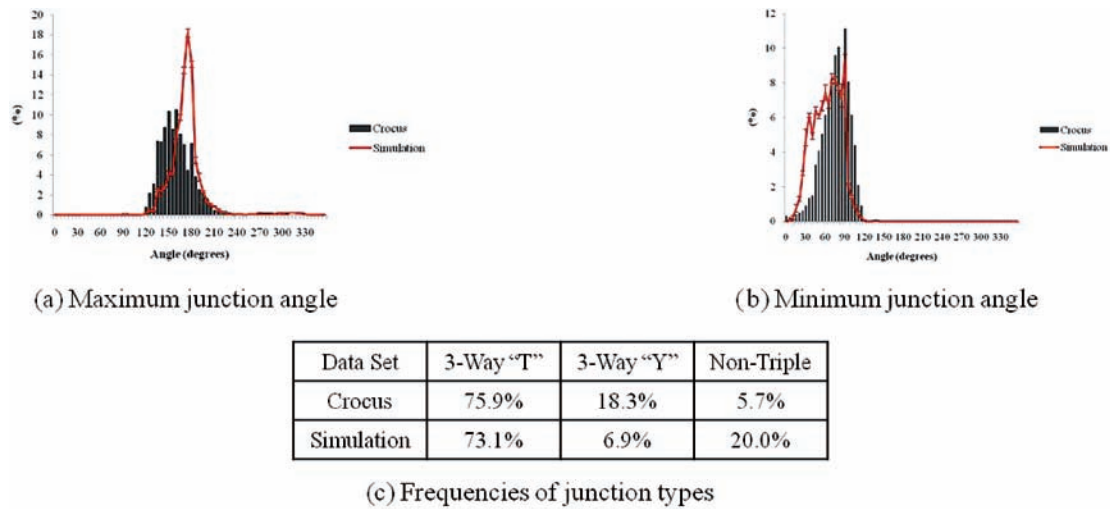


Fig. 10. Comparison of junction properties.

observed in other domains using time-lapsed photography (e.g., desiccation of clay [Tang and Shi 2008]). Our contribution is mainly to argue for it statistically.

6. CONCLUSION AND FUTURE WORK

In this article, we have described methods to analyze the fracture patterns observed in a manually reconstructed wall painting. We describe an interactive program to trace detailed fragment boundaries in images and geometric analysis algorithms to produce statistical distributions of lengths, angles, areas, and adjacencies found in the traced fragment arrangements. From this study, we find that (1) fragments tend to be nearly convex polygons with 3–8 sides, (2) the distribution of fragment areas roughly follows an exponential distribution, (3) “edges” between two adjacent fragments tend to be nearly straight, and (4) “junctions” most often appear with three fragments coming together in a T-junction. These observations suggest a hierarchical fracture pattern where fragments break recursively into two nearly equal-size pieces along cracks nearly orthogonal to previous ones. We provide evidence for this model by means of comparison with simulation results of a hierarchical fracture process.

While this study takes a small step, our approach has several limitations and there are many avenues for future research. As a next step, future work should perform analysis of many different wall paintings and ideally many different artifact types. Although our dataset has over 4,000 fragments, they are all from the same wall painting, and so it may not be representative of other wall paintings or other artifacts made from different materials. We conjecture that our main conclusions generalize to other fractured artifacts constructed from brittle materials, but further study is required to confirm this hypothesis. More broadly, we think that the methodologies used in this study could be useful in a variety of archaeological settings where analysis of fracture patterns may yield interesting information about how an artifact was constructed or broken. For example, it would be interesting to study whether different materials or causes of failure produce different types of fracture patterns. We plan to gather more data and to make our tools publicly available so that analysis and comparison of different archaeological artifacts can be performed in the future.

A second interesting topic for future work is to utilize the observed statistics and fracture model presented in this article to guide computer-assisted reconstruction algorithms. Funkhouser et al. [2011]

make a step toward this goal by incorporating features inspired by these statistics in a machine learning approach to find pairwise matches of fragments. However, there is much room for further possibilities, and exploring them fully is still a topic for future work.

Finally, the proposed hierarchical fracture model could be confirmed with high speed video, as was done for fracture under biaxial loading in Olson [2007].

REFERENCES

- BAZIN, P.-L. AND HENRY, A. 2003. Wall drawer: A simple solution to traditional drawing and photographic recording of archaeological features. *J. Field Archaeology*.
- BHANDARKAR, S., ROBINSON, R., AND YU, J. 2009. Virtual multi-fracture craniofacial reconstruction using computer vision and graph matching. *Computerized Medical Imag. Graph.* 33, 333–342.
- BOHN, S., DOUADY, S., AND COUDER, Y. 2005a. Four sided domains in hierarchical space dividing patterns. *Phys. Rev. Lett.* 94, 5, 054503.
- BOHN, S., PAUCHARD, L., AND COUDER, Y. 2005b. Hierarchical crack patterns as formed by successive domain divisions. *Phys. Rev. E* 71, 4, 046214.
- BROWN, B., TOLER-FRANKLIN, C., NEHAB, D., BURNS, M., DOBKIN, D., VLACHOPOULOS, A., DOUMAS, C., RUSINKIEWICZ, S., AND WEYRICH, T. 2008. A system for high-volume acquisition and matching of fresco fragments: Reassembling Theran wall paintings. *ACM Trans. Graph.* 27, 3.
- CAWSEY, D. C. 1977. The measurement of fracture patterns in the chalk of southern England. *Engin. Geology* 11, 3, 201–215.
- CLOOS, E. 1955. Experimental analysis of fracture patterns. *Geological Soc. Amer.* 66, 3, 241–256.
- COOPER, D., WILLIS, A., ANDREWS, S., BAKER, J., CAO, Y., HAN, D., KANG, K., KONG, W., LEYMARIE, F., ORRIOLS, X., VELIPASALAR, S., VOTE, E., JOUKOWSKY, M., KIMIA, B., LAIDLAW, D., AND MUMFORD, D. 2001. Assembling virtual pots from 3d measurements of their fragments. In *Proceedings of the Conference on Virtual Reality, Archeology, and Cultural Heritage (VAST '01)*. ACM, New York, NY, 241–254.
- DEMAINE, E. AND DEMAINE, M. 2007. Jigsaw puzzles, edge matching, and polyomino packing: Connections and complexity. *Graph. Comb.* 23, 1, 195–208.
- DOUMAS, C. 1992. *The Wall-Paintings of Thera*. Thera Foundation, Athens, Greece.
- FREEMAN, H. AND GARDER, L. 1964. Apictorial jigsaw puzzles: The computer solution of a problem in pattern recognition. *IEEE Trans. Electron. Comput.* EC-13, 2, 118–127.
- FUNKHOUSER, T., SHIN, H., TOLER-FRANKLIN, C., CASTAÑEDA, A. G., BROWN, B., DOBKIN, D., RUSINKIEWICZ, S., AND WEYRICH, T. 2011. Learning how to match fresco fragments. In *Proceedings of the Eurographics Area Track on Cultural Heritage*.
- GOLDBERG, D., MALON, C., AND BERN, M. 2004. A global approach to automatic solution of jigsaw puzzles. *Computat. Geometry: Theory Appl.* 28, 2-3, 165–174.
- GRIFFITH, A. 1921. The phenomena of rupture and flow in solids. *Philosophical Transa. Royal Soc. London A* 221, 163–198.
- HANDGE, U. 2002. Analysis of a shear-lag model with nonlinear elastic stress transfer for sequential cracking of polymer. *J. Materials Science* 37, 22, 4775–4782.
- HUANG, Q., FLÖRY, S., GELFAND, N., HOFER, M., AND POTTMANN, H. 2006. Reassembling fractured objects by geometric matching. *ACM Trans. Graph.* 25, 3, 569–578.
- IBEN, H. AND O'BRIEN, J. 2009. Generating surface crack patterns. *Graphical Models* 71, 6, 198–206.
- KARASIK, A. AND SMILANSKY, U. 2008. 3d scanning technology as a standard archaeological tool for pottery analysis: practice and theory. *J. Archaeol. Sci.* 35, 1148–1168.
- KLEBER, F., DIEM, M., AND SABLATNIG, R. 2009. Torn document analysis as a prerequisite for reconstruction. In *Proceedings of the 15th International Conference on Virtual Systems and Multimedia (VSMM '09)*. IEEE Computer Society, Los Alamitos, CA, 143–148.
- KOLLER, D. AND LEVOY, M. 2006. Computer-aided reconstruction and new matches in the forma urbis romae. *Bullettino Della Commissione Archeologica Comunale di Roma* 15, 103–125.
- KORNETTA, W., MENDIRATTA, S., AND MENTEIRO, J. 1998. Topological and geometrical properties of crack patterns produced by the thermal shock in ceramics. *Phys. Rev. E* 57, 3, 3142–3152.
- LACHENBRUCH, A. 1962. Mechanics of thermal contraction cracks and icewedge polygons in permafrost. *Geological Soc. Amer. Spec* 70, 7, 69.
- LEITÃO, H. AND STOLFI, J. 2002. A multiscale method for the reassembly of two-dimensional fragmented objects. *IEEE Trans. Pattern Analy. Machine Intell.* 24, 9, 1239–1251.

- LEITÃO, H. AND STOLFI, J. 2005. Measuring the information content of fracture lines. *Int. J. Computer Vision* 65, 3, 163–174.
- MCBRIDE, J. AND KIMIA, B. 2003. Archaeological fragment reconstruction using curve-matching. In *Proceedings of the Computer Vision and Pattern Recognition Workshop 1*, 3.
- MCDANELS, S., MAYEAUX, B., AND RUSSELL, R. 2006. An overview of the space shuttle columbia accident from recovery through reconstruction. *J. Failure Anal. Preven.* 6, 1, 82–91.
- MORTENSEN, E. N. AND BARRETT, W. A. 1995. Intelligent scissors for image composition. In *Proceedings of the 22nd Annual Conference on Computer Graphics and Interactive Techniques (SIGGRAPH '95)*. ACM, New York, NY, 191–198.
- MULHERAN, P. 1993. Crack networks in thin films. *Philosophical Mag. Lett.* 68, 2, 63–68.
- OLSON, J. 2007. Fracture aperture, length and pattern geometry development under biaxial loading: A numerical study with applications to natural, cross-jointed systems. In *The Fracture-Like Damage and Localisation.*, The Geological Society of London, 123–142.
- PAPAIOANNOU, G. AND KARABASSI, E. 2003. On the automatic assemblage of arbitrary broken solid artefacts. *Image and Vision Comput.* 21, 5, 401–412.
- PAPANDREOU, G. 2009. Image analysis and computer vision: Theory and applications in the restoration of ancient wall paintings. Ph.D. thesis, National Technical University of Athens, Greece.
- PAPAODYSSSEUS, C., PANAGOPOULOS, M., ROUSOPOULOS, P., GALANOPOULOS, G., AND DOUMAS, C. 2008. Geometric templates used in the Akrotiri (Thera) wall-paintings. *Antiquity* 82, 316, 401–408.
- PAPAODYSSSEUS, C., PANAGOPOULOS, T., AND EXARHOS, M. 2002. Contour-shape based reconstruction of fragmented, 1600 B.C. wall paintings. *IEEE Trans. Signal Process.* 50, 6, 1277–1288.
- RATS, M. V. 1968. *Nonuniformity of Rocks and Their Physical Properties* [in Russian]. Nauka, Moscow, Russia.
- SHIN, H., DOUMAS, C., FUNKHOUSER, T., RUSINKIEWICZ, S., STEIGLITZ, K., VLACHOPOULOS, A., AND WEYRICH, T. 2010. Analyzing fracture patterns in Thera wall paintings. In *Proceedings of the 11th International Symposium on Virtual Reality, Archaeology and Cultural Heritage (VAST)*.
- TANG, C. AND SHI, B. 2008. Influencing factors of geometrical structure of surface shrinkage cracks in clayey soils. *Engin. Geology* 101, 3-4.
- TOLER-FRANKLIN, C., BROWN, B., WEYRICH, T., FUNKHOUSER, T., AND RUSINKIEWICZ, S. 2010. Multi-feature matching of fresco fragments. Tech. rep. TR-874-10, Department of Computer Science, Princeton University.
- TSYGANKOV, S. 2000. On preferred dimensions and shapes of blocks. *J. Min. Science* 36, 1, 30–36.
- VLACHOPOULOS, A. 2007. The wall paintings from the Xeste 3 building at Akrotiri: Towards an interpretation of the iconographic programme. In *Proceedings of the a Colloquium on the Prehistory of the Cyclades*. 491–505.
- WILLIS, A. AND COOPER, D. 2008. Computational reconstruction of ancient artifacts. *IEEE Signal Proces. Mag.* 25, 4, 65–83.

Received July 2011; revised November 2011; accepted January 2012